Hindawi
International Journal of Polymer Science
Volume 2023, Article ID 8844626, 8 pages
https://doi.org/10.1155/2023/8844626

Research Article

Surface Roughness Modeling of Material Extrusion PLA Flat Surfaces

Kaltrine Jakupi,[1,2] **Vladimir Dukovski**,[2] **and Gezim Hodolli**[3]

[1]*Faculty of Mechanical Engineering, University in Prishtina "Hasan Prishtina", St. "George Bush", Nr. 31, Pristina 10000, Kosovo*
[2]*Faculty of Mechanical Engineering, Ss. Cyril and Methodius University in Skopje, P.O. Box 464, Skopje MK-1001, North Macedonia*
[3]*Faculty of Veterinary and Agriculture, University in Prishtina "Hasan Prishtina", St. "George Bush", Nr.31, Pristina 10000, Kosovo*

Correspondence should be addressed to Gezim Hodolli; gezim.hodolli@uni-pr.edu

Received 23 March 2023; Revised 3 May 2023; Accepted 5 May 2023; Published 13 May 2023

Academic Editor: Joanna Rydz

Complex forms may be easily created with additive manufacturing methods, but managing surface roughness remains a difficulty, even for flat surfaces, because surface quality is dependent on numerous parameters. This research investigates the effect of some printing factors on surface roughness in 3D printing methods. The purpose of this study is to quantify the most influential input printing factors on surface roughness in 3D printing processes. Polyacrylic acid thermoplastic was used to print workpieces, and mathematical models were generated using the regression method to analyze the relationship between process parameters and surface roughness. The exponential model fits the experimental data slightly better than the linear model. Only Ra-90 met all surface roughness classification requirements, while surface roughness measurements in the 0 and 45-degree directions did not meet the requirements and cannot be used to describe the surface roughness. The study highlights the importance of considering input printing parameters when optimizing surface roughness in 3D printing processes, providing valuable insights into the impact of process parameters on surface roughness.

1. Introduction

Fused deposition modeling (FDM) is the most frequently used three-dimensional (3D) printing technology, and it can be used to produce workpieces by extruding thermoplastic filaments. The workpieces first need to be designed using computer-aided design (CAD) and then converted as STL (stereo-lithography) files to G-code, which contains enough instructions to print out the physical object as designed [1]. Figure 1 illustrates the 3D manufacturing process with FDM technology.

Many sectors employ 3D printing technologies, like aerospace [2], medicine [3], dental implants [4], education [5], energy [6], and automotive [7]. Furthermore, as Kechagias points out in his editorial [8], there are many more specific applications for materials and products based on additive manufacturing that have excellent physical and mechanical properties.

3D printing produces a physical workpiece with a complex shape by heating the plastic and forming it into layers that are placed one after the other [9]. Because of its low cost, varied production, shorter process time, and ease of use, this technology has now become increasingly applied.

Workpieces are determined by a multitude of parameters, which must be chosen as the correct parameters to prepare the models that will print [10]. The workpieces constructed of polyacrylic acid (PLA) thermoplastic were manufactured using FDM technology.

Surface texture is important since it has a direct influence on the quality of the parts. Unfiltered profiles are the ones that are directly measured over workpiece material in two dimensions (P-profile). Filtering is performed following ISO 16610-21 [11], for the waviness (W-profile) and roughness profiles (R-profile).

For this study, the surface roughness of arithmetic means deviation parameters were measured and represented by Ra, and it was measured in three different directions related to printing directions, 0, 45, and 90 degrees. ISO 21920-2 [12] specifies the Ra parameter and its definitions.

Figure 1: Basic steps of the FDM process for 3D printing.

The microscopic asperity of the surface of each workpiece has a significant impact on surface roughness. Many studies have been published regarding the surface roughness of thermoplastic workpieces and their relation with input parameters [13, 14].

The printing input parameters impact the surface roughness of workpieces, and the Taguchi [15] method was used instead of the full factorial method for a systematic approach to optimize the process for performance, quality, and cost [15]. The theoretical models were then generated using the multi-regression approach.

The main theme of this work is the Ra modeling of flat PLA-Fused Filament Fabrication parts variating three key parameters in three different directions (0, 45, and 90 degrees from strands). The models were generated based on layer height, printing speed, and infill percentage, to enhance the quality of 3D-printed items. In addition, this study thoroughly examined the advantages of utilizing both linear and exponential modeling approaches.

2. Experimental Methodology

2.1. Design of Experiment. By utilizing the Taguchi method, the number of runs and combinations of values were designed for three chosen independent parameters, each with three levels. This approach enabled us to gather sufficient data with only partial experiments, streamlining the research process while maintaining the quality of the results [16].

Layer height, print speed, and infill percentages were selected as independent parameters. For each independent parameter, three levels were chosen to optimize the surface roughness: lowest, median, and maximal values. While software constantly recommends the medium level. This level range enables more accurate and effective optimization, resulting in a higher-quality end product.

The layer height parameter determines the thickness of each printed layer and has a significant effect on the final surface quality. The lowest layer thickness for this experiment was 0.1 mm and it increased by 0.05 mm, so the second and third levels were 0.15 and 0.2 mm.

The print speed parameter affects the time between each layer being deposited, which can influence the degree of melting and cooling of the material and ultimately impact surface roughness. The slowest level of print speed parameter was 70 mm/s, the moderate print speed was 80 mm/s, and the fastest print speed was 90 mm/s.

The infill percentage parameter determines the amount of material deposited within the printed structure and can have a significant effect on the overall strength and stability of the print. The aim of optimizing these parameters is to achieve the desired surface roughness for the specific application. The lowest infill percentages were 30%, then the second and third level of infill percentages were 40% and 50%.

To conduct accurate theoretical modeling of 3D printing processes, it is important to consider the effect of layer thickness on surface roughness. Previous studies have shown that layer thickness can significantly impact the quality and resolution of the printed part, even on the top face [17, 18].

For this case, nine runs with the specific combination were prepared. The same parameter and run combinations as listed in Table 1.

2.2. Multiple Regression Analysis. Multiple regression is a technique for determining one dependent variable from independent variables. The arithmetic means deviation (Ra) was utilized as a dependent value in this research to categorize surface roughness on the top side of 3D-printed workpieces, whereas the factors (thickness, print speed, and infill percentage) were used as independent variables. As a consequence, the dependent variable may theoretically be expressed as a linear or exponential model, which is used to identify the relationship between the dependent variable and the independent variables.

$$R_a = \beta_o + \beta_1 T_h + \beta_2 P_s + \beta_3 I_d, \quad (1)$$

$$R_a = \beta_0 T_h^{\beta_1} P_s^{\beta_2} I_d^{\beta_3}, \quad (2)$$

where: β_0, β_1, β_2, and β_3 are regression coefficients, independent variables: T_h—thickness, P_s—print speed, and I_d—infill percentage. The least squares approach was used to estimate the exponential coefficients of equation (2).

2.3. The Filament and Printer Calibration. The workpieces were designed and printed in the same manner, with dimensions of (40 × 40 × 20) mm. For PLA thermoplastic, the nozzle diameter was 0.4 mm, with nozzle and bed temperatures 200°C and 60°C, respectively. The shell number was 2, and the slicer software "PrusaSlicer" can automatically update it if needed.

This research was carried out by a commercial 3D printer named "Original Prusa i3 MK3S+". The printer was calibrated following the printer manufacturer's instructions.

2.4. Surface Roughness Parameters and Testing Equipment. To quantify the surface roughness of workpieces, Ra was chosen. The roughness average (Ra) is the arithmetic average of the absolute values of the profile heights over the evaluation

Table 1: The independent variables and combinations of three levels utilized to print specific workpiece runs.

Runs	Coded factors			Independent/input parameters			Dependent/measured parameter [μm]		
	X_1	X_2	X_3	T_h (mm)	P_s (mm/s)	I_d (%)	Ra-0	Ra-45	Ra-90
1	1	1	1	0.1	70	30	2.99	8.52	12.04
2	1	2	2	0.1	80	40	2.13	8.81	13.02
3	1	3	3	0.1	90	50	2.92	8.97	14.08
4	2	1	2	0.15	70	40	4.28	9.21	15.01
5	2	2	3	0.15	80	50	3.26	9.25	15.35
6	2	3	1	0.15	90	30	1.52	9.77	16.22
7	3	1	3	0.2	70	50	1.64	9.68	15.31
8	3	2	1	0.2	80	30	1.50	9.53	17.24
9	3	3	2	0.2	90	40	1.57	9.61	18.14

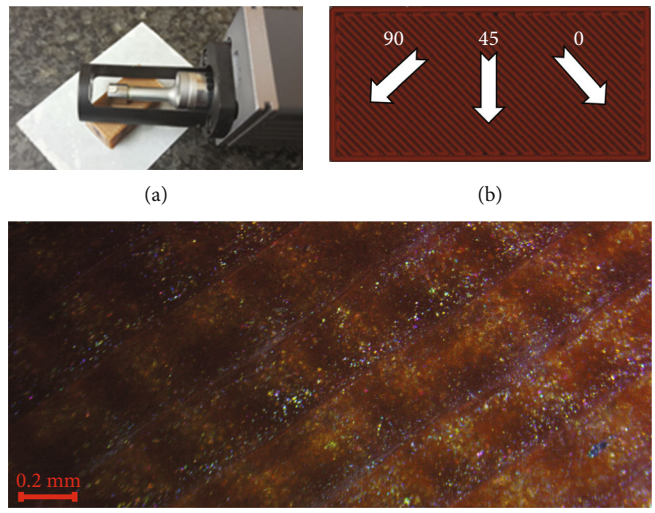

(a) (b) (c)

Figure 2: Measuring process of the top layer of printed workpieces. (a) Ra-90 measuring process, (b) measuring orientation related to printing lines of the top face, and (c) the surface of workpiece number one scanned by optical microscope.

length. The spectrometer Hadron SRT-6210 by Metorex Arcmet 930 was used for measuring Ra as dependent values.

The surface roughness device was set up to measure the evaluation length at 4 mm, with steps measuring 0.5 μm and 0.5 mm/s for speed. So, for each measurement of the Ra profile, 8000 data points were collected and exported for further calculations.

3. Results and Discussion

No post-processing techniques were applied on the workpieces' top surfaces, which is the latest printed layer of the workpiece. The printing direction was set at 45 degrees by default to the workpiece orientation, and the layers for each slice alternately changed to 90 degrees. Figure 2(a) shows the measurement process of the top layer for printed workpieces at 90 degrees; Figure 2(b) shows the three-direction measurement: Ra-0, Ra-45, and Ra-90, which are related to the printing directions of workpieces; and Figure 2(c) shows the surface of workpieces scanned by optical microscope.

To verify the measuring device's quality control, the standard was first measured, known as a "precision reference specimen" with 130620 as the code and identification number. The standard's Ra profile must give Ra = 3.10 μm, and the measurement direction must be at 90 degrees to the direction of its printed line. The sub-graph (a) of Figure 3 shows the profiles of nine workpieces measured at 0 degrees to the printing direction. The oscillation of Ra profiles was between −20 and 20 μm.

The sub-graph (b) of Figure 3 shows the profiles of nine workpieces measured at 45 degrees to the printing direction. The oscillation of Ra profiles is between −30 and 30 μm. Graph (c) of Figure 3 shows the profiles of nine workpieces measured at 90 degrees to the printing direction. The range of oscillation is the same as the graph in (b). The sub-graph (d) of Figure 3 shows the profile of the standard. The graph's periodicities indicate the measurement device's quality.

Ten measurements of Ra were done in the top face of workpieces, then the average of the batch was determined for comparison purposes: 0, 45, and 90 degrees; the average was indicated in red in Figure 3. The average of Ra for 0 and 45-degree observations revealed no periodicity; 0-degree

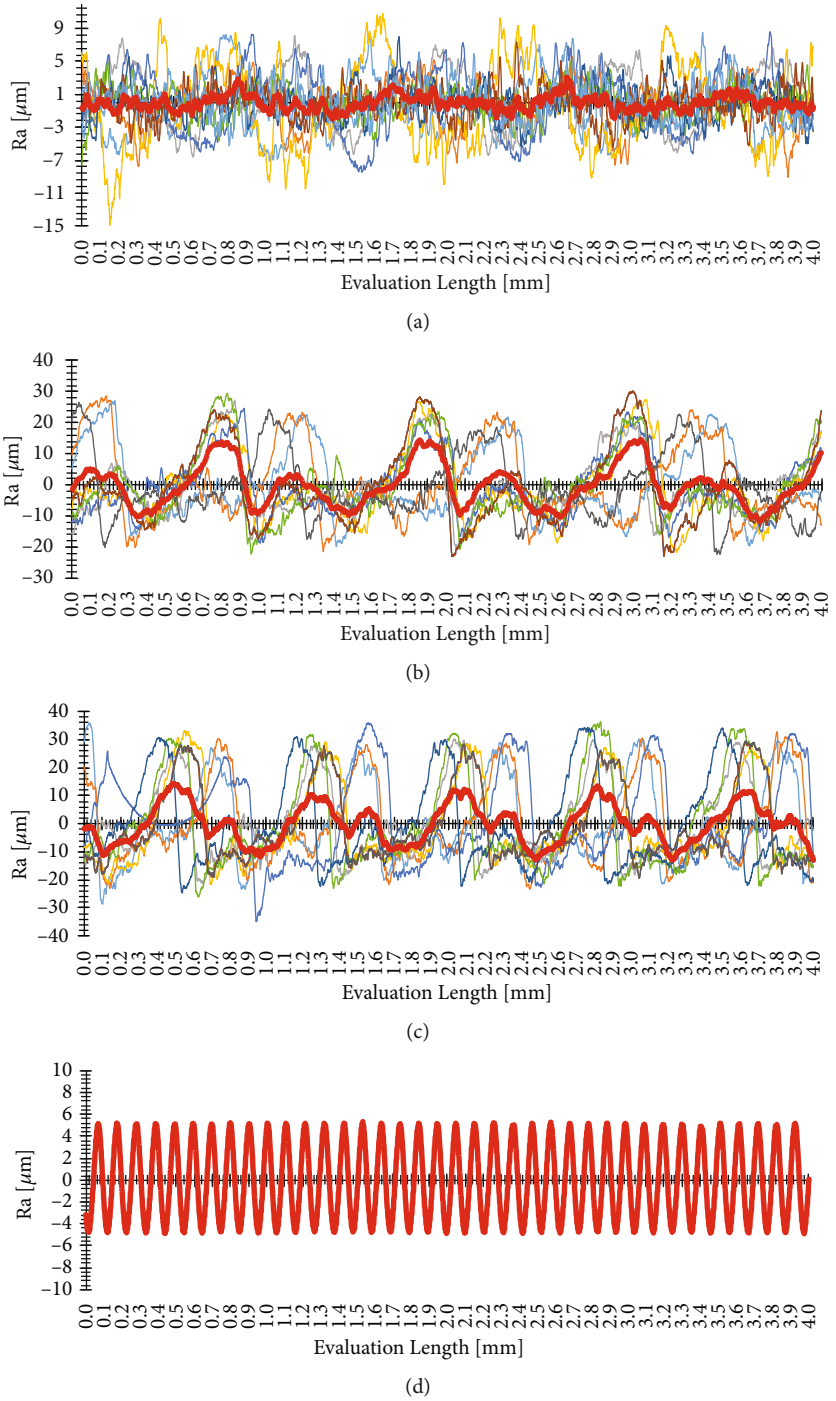

Figure 3: The measured Ra profiles (a) for nine runs of PLS at 0 degrees, (b) for nine runs of PLS at 45 degrees, (c) for nine runs of PLS at 90 degrees, and (d) for the standard precision reference specimen.

graphs showed no periodicity at all, while 45-degree graphs showed periodicity only in the second half of the graph. The best periodicity was achieved from observations at 90 degrees; this was continuous across all of the graph lengths.

Equations (1) and (2) were utilized to obtain the optimum mathematical models. As a result, the Ra surface roughness of PLA thermoplastic is theoretically computed for linear and exponential models. Table 2 lists theoretical model equations and statistical data. Theoretical models were created based on measurements of the top surface of workpieces and cannot be applied to vertical or sloping surfaces of workpieces.

For linear and exponential models of Ra-0 degrees, the ANOVA p-value was 0.306 and 0.232, and they should be less than 0.05. As a result, the models containing independent variables fail to explain the dependent variable. The findings from those models are not statistically significant.

For Ra-45 and Ra-90 degrees, theoretical models reveal a substantial link between independent and dependent variables.

Table 2: The linear and exponential models, as well as the statistical data for 0, 45, and 90 degrees of observed orientation concerning PLA thermoplastic printing lines.

Degree	Theoretical model*	Multiple R	R Square	Standard Error	ANOVA p-value
0	$R_{a0} = 6.748 - 11.1T_h - 0.048P_s + 0.031I_d$	0.70	0.48	0.89	0.306
	$R_{a0} = 47.031T_h^{-0.699}P_s^{-1.468}I_d^{0.555}$	0.74	0.54	0.34	0.232
45	$R_{a45} = 6.694 + 8.4T_h + 0.015P_s + 0.002I_d$	0.90	0.82	0.23	0.025
	$R_{a45} = 6.489T_h^{0.135}P_s^{0.135}I_d^{0.007}$	0.92	0.86	0.02	0.014
90	$R_{a90} = 1.781 + 38.5T_h + 0.101P_s - 0.013I_d$	0.98	0.95	0.52	0.001
	$R_{a90} = 3.078T_h^{0.376}P_s^{0.535}I_d^{-0.008}$	0.98	0.97	0.03	<0.001

*Those parameters were defined in Section 2.2, specifically on equations (1) and (2).

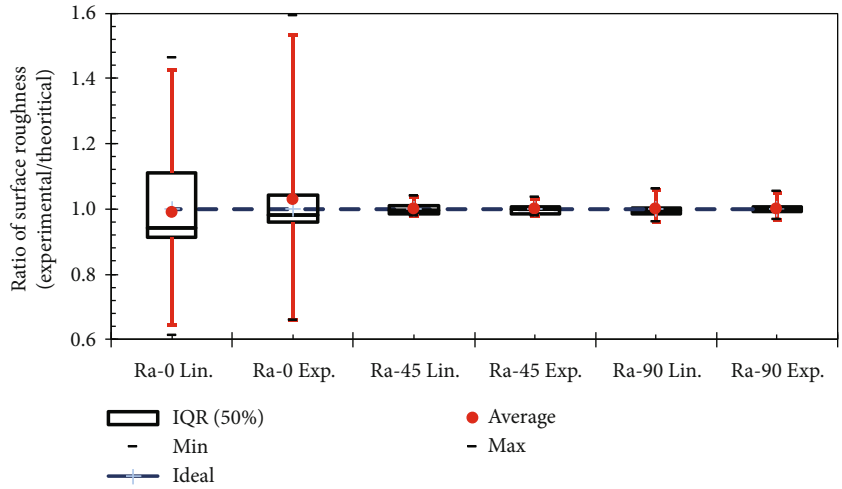

Figure 4: Distributions of the ratio between experimental/theoretical results for linear and exponential models of studied directions.

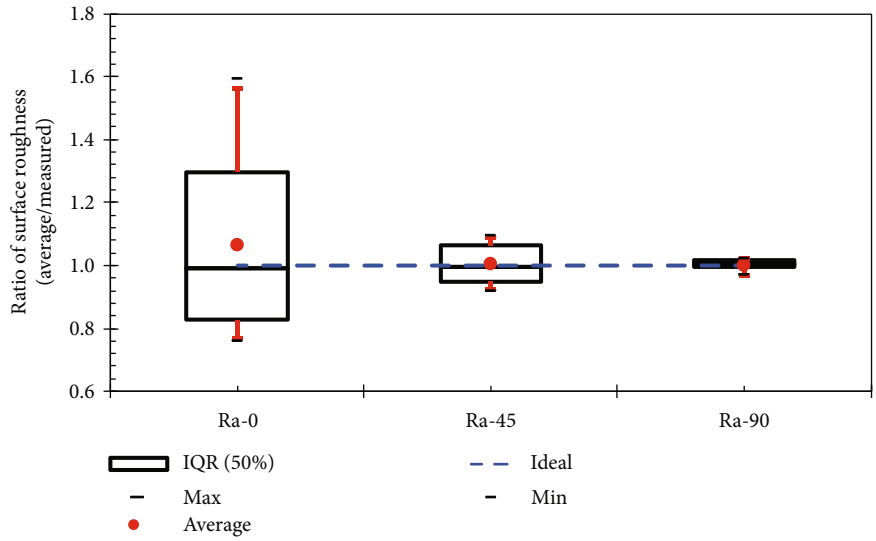

Figure 5: The repeatability of surface roughness Ra-0, Ra-45, and Ra-90 degrees, $n = 10$.

The significance F was less than the alpha value for both models. As a result, there was substantial evidence that the linear and exponential regression models were statistically significant.

The majority of statistical coefficients were nearly identical for linear and exponential models between the same batches of measurement degree to printed orientation, with both models demonstrating a significant correlation. The exponential model had a little advantage for Ra-45 and Ra-90 degrees. In addition, both theoretical models demonstrated similarities in estimated points on the regression line, as assessed by R square in Table 2.

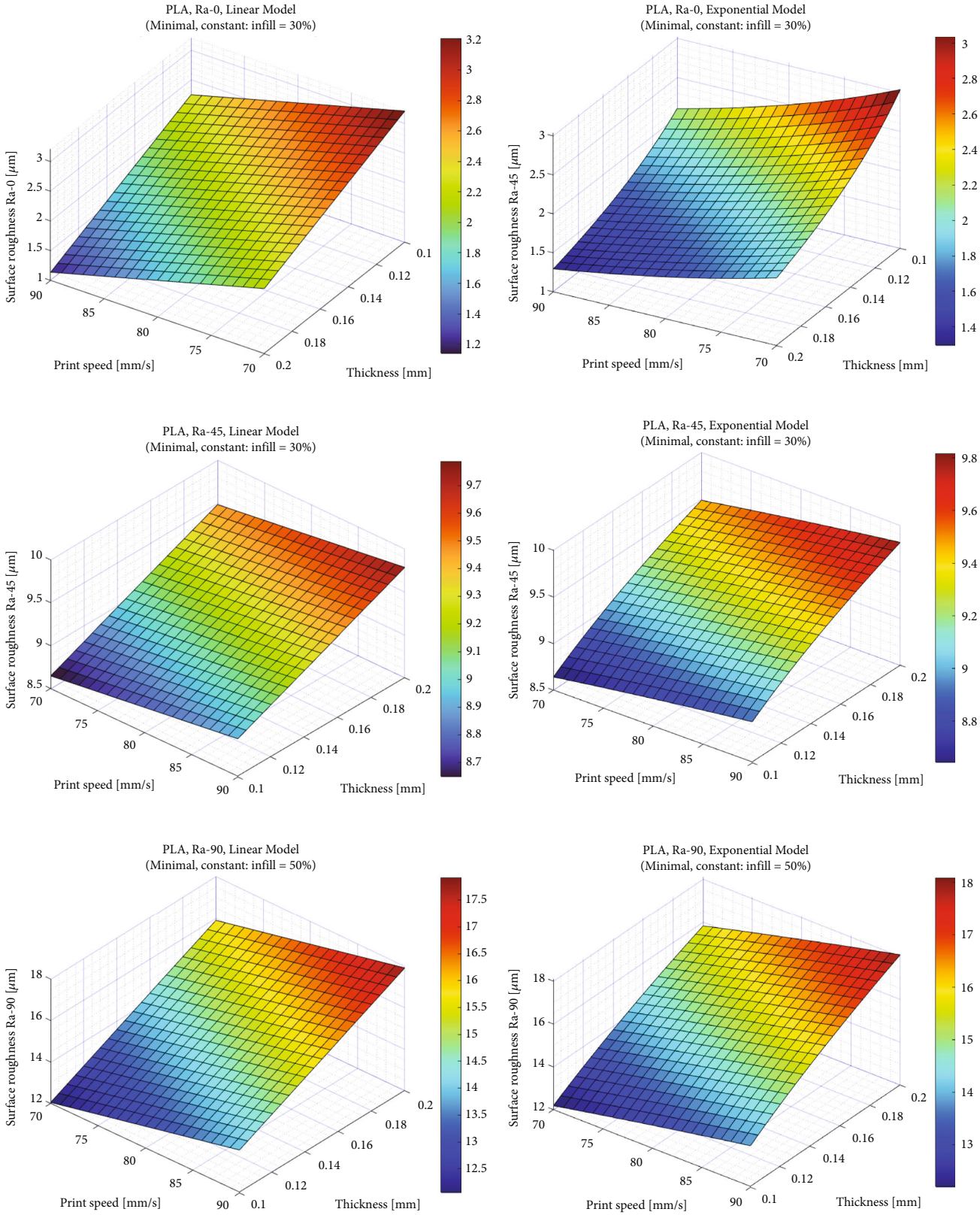

Figure 6: Calculated minimal values of surface roughness (Ra-0, Ra-45, and Ra-90) for linear and exponential modeling for workpieces of the top face made by PLA.

The signs of the independent parameters were exactly identically for the same batches under study, demonstrating the similarity of parameters significance between the linear and exponential models. Because their p-values were less than alpha, all independent variables in both models for 45 degrees showed a significant correlation with surface roughness. The theoretical model's most significant parameter was layer thickness.

The thickness received p-values smaller than 0.05 for theoretical models at 90 degrees. The remainders of the independent variables pass the p-value test.

The surface roughness ratio R was calculated to compare measured and theoretical model data, and the findings are displayed in Figure 4. The red circle indicates the mean value, the box indicates the 50% range, the vertical red line indicates the 90% range, the horizontal red line within the box indicates the median, and the extreme black lines outside the box indicate the minimum and maximum values.

The practical-to-theoretical distribution ratio for Ra-0 is several orders of magnitude higher than the ratio results for Ra-45 and Ra-90. Furthermore, both models' Ra-45 and Ra-90 distributions are very close to the ideal line.

The surface roughness's Ra-0, Ra-45, and Ra-90 of the same workpiece were measured 10 times to establish consistency of the results; the same experiment, with the same equipment, must provide the same results. The ratio coefficient of surface roughness was calculated by dividing the average measured result for specific surface roughness by the measured result. Figure 3 shows the statistical distributions of surface roughness.

The repeatability test quality was categorized depending on the orientation of the workpiece measurement. Randomly chosen workpiece number one was measured 10 times for R-0, R-45, and R-90. The distribution of the results was as follows.

On repetition of measurements, the surface roughness Ra-0 distribution was up to 24% less and 60% more than the average of the batch. Because of the high sensitivity of the measurement device during setup, Ra-0 has a high level of uncertainty. The surface roughness Ra-45 distribution was up to 9.3% less and 8.9% greater than the batch average. Also, this range is thought to be too broad to be utilized for assessing surface roughness. The distribution of surface roughness Ra-90 was up to 3% less and up to 2% higher than the average, 95% of results were within 2–3% away of the target. Therefore, surface roughness Ra-90 can be used to quantify the quality of the surface. The probability of measurement for Ra-90 indicates a 95% coverage level. Figure 5 shows graphically the results.

Based on repeatability tests, only Ra-90 was consistent in measuring the surface roughness. Similar results were reported by Banjanin et al. [19]. The Ra-0 and Ra-45 were useless due to the high uncertainty of the measuring device.

Also, the purpose of this research is to find the extreme value of surface roughness for a given set of independent variables. So, 3D graphs for linear and exponential models of Ra-90 were generated and presented in Figure 6.

The range of surface roughness Ra-90 for three independent variables and three levels of values for linear and exponential models were from 12.09 up to 14.37 μm and 12.21 up to 14.03 μm, respectively.

Based on the experimental and theoretical data of this study, can conclude that there was a significant correlation between surface roughness and the input parameters investigated in this study for Ra-90. The parameter that has the highest impact on surface roughness is layer height, followed by print speed, and lastly, infill percentage has the smallest impact.

The surface roughness increases significantly with the increase in layer thickness. This is because thicker layers can create more visible layer lines, which can contribute to the roughness of the surface. In general, a thinner layer height will result in a smoother surface finish, but it will also increase the print time.

A similar mechanism in surface roughness was also observed with the print speed parameter. If the print speed is too high, the extruded material may not have enough time to properly bond to the previous layer, resulting in a rougher surface finish. An optimized print speed for the specific printer and filament being used can help achieve a smoother surface finish.

Unlike the previous two factors, the infill percentage had a significantly lesser effect. Surface roughness reduces when the infill percentage value is increased. This is due to a larger infill percentage providing more support for the 3D-printed part's outer layers, resulting in a smoother surface finish.

4. Conclusions

Based on the measurement results and the implemented modeling, the independent parameters can be ranked in order of significance for surface roughness, from highest to lowest: layer height, print speed, and infill percentage. It has been demonstrated that the surface roughness increases with the increase of layer height and print speed values. Conversely, it decreases with the increase in infill percentage.

However, due to significant uncertainty in repeatability, surface roughness Ra-0 and Ra-45 were deemed unreliable for estimating surface roughness. Nevertheless, both mathematical models effectively predicted surface roughness for Ra-90.

The linear model of Ra-90 generated a surface roughness range of 14.37–18.22 μm, while the exponential model generated a range of 14.03–18.21 μm. In comparison to the linear model for Ra-90, the exponential mathematical model proved to be a better fit for the experimental data.

So, adjusting the input parameters such as infill percentage, print speed mm/s, and layer height can impact the surface roughness of PLA parts printed from a 3D printer. By optimizing these parameters, it is possible to achieve a smoother surface finish, but it is important to balance this with other factors such as print time and part strength.

Data Availability

Data supporting this research article are available from the corresponding author or first author on reasonable request.

Conflicts of Interest

The authors declare that they have no conflicts of interest.

Authors' Contributions

VD: conceptualization and experimental design, KJ: experimental design and carrying out measurements, GH: theoretical models and manuscript composition.

Acknowledgments

The authors would like to thank the Faculty of Mechanical Engineering University of Pristina "Hasan Prishtina" for supporting to carry out this work.

References

[1] G. Rasiya, A. Shukla, and K. Saran, "Additive manufacturing—a review," *Materials Today: Proceedings*, vol. 47, pp. 6896–6901, 2021.

[2] B. Blakey-Milner, P. Gradl, G. Snedden et al., "Metal additive manufacturing in aerospace: a review," *Materials and Design*, vol. 209, p. 110008, 2021.

[3] J. Kaltrine, V. Gligorče, D. Vladimir, and H. Gezim, "Design and manufacturing of 3D printed parts for radiotherapy application," *Journal of Mechanical Engineering Science*, vol. 40, pp. 11–15, 2022.

[4] J. D. Kechagias and S. P. Zaoutsos, "Optimising fused filament fabrication surface roughness for a dental implant," *Materials and Manufacturing Processes*, vol. 38, pp. 954–959, 2023.

[5] F. F. Ramdhani and B. Mulyanti, "Additive manufacturing in education," *IOP Conference Series: Materials Science and Engineering*, vol. 830, p. 42093, 2020.

[6] C. L. Cramer, E. Ionescu, M. Graczyk-Zajac et al., "Additive manufacturing of ceramic materials for energy applications: road map and opportunities," *Journal of the European Ceramic Society*, vol. 42, pp. 3049–3088, 2022.

[7] V. Mohanavel, K. S. Ashraff Ali, K. Ranganathan et al., "The roles and applications of additive manufacturing in the aerospace and automobile sector," *Materials Today: Proceedings*, vol. 47, pp. 405–409, 2021.

[8] J. D. Kechagias, "Materials for additive manufacturing," *AIMS Materials Science*, vol. 9, pp. 785–790, 2022.

[9] I. Gibson, D. W. Rosen, and B. Stucker, *Additive Manufacturing Technologies*, pp. 7–26, Springer, US, Boston, MA, 2010.

[10] J. Kechagias and D. Chaidas, "Fused filament fabrication parameter adjustments for sustainable 3D printing," *Materials and Manufacturing Processes*, vol. 38, pp. 933–940, 2023.

[11] International Organization for Standardization, 2011, ISO 16610-21:2011(en), Geometrical Product Specifications (GPS)—filtration—part 21: linear profile filters, Gaussian filters. https://www.iso.org/obp/ui/#iso:std:iso:16610:-21:ed-1:v1:en, accessed 8 Nov 2022.

[12] International Organization for Standardization ISO 21920-2:2021 Geometrical Product Specifications (GPS)—surface texture: profile—part 2: terms, definitions and surface texture parameters. https://www.iso.org/standard/72226.html, accessed 8 Nov 2022.

[13] M. Nalbant, H. Gökkaya, and G. Sur, "Application of Taguchi method in the optimization of cutting parameters for surface roughness in turning," *Materials and Design*, vol. 28, pp. 1379–1385, 2007.

[14] D. Chaidas and J. D. Kechagias, "An investigation of PLA/W parts quality fabricated by FFF," *Materials and Manufacturing Processes*, vol. 37, pp. 582–590, 2022.

[15] R. K. Roy, *A Primer on the Taguchi Method*, pp. 23–129, Society of Manufacturing Engineers, Dearborn, MI, 2nd edition, 2010.

[16] M.-D. Jean and Y.-F. Tzeng, "Use of Taguchi methods and multiple regression analysis for optimal process development of high energy electron beam case hardening of cast iron," *Surface Engineering*, vol. 19, pp. 150–156, 2003.

[17] N. Ayrilmis, "Effect of layer thickness on surface properties of 3D printed materials produced from wood flour/PLA filament," *Polymer Testing*, vol. 71, pp. 163–166, 2018.

[18] A. Dandgawhal, A. Shukla, C. Ranade et al., "Experimental studies on effect of layer thickness on surface finish using FDM," *International Research Journal of Engineering and Technology (IRJET)*, vol. 9, no. 6, pp. 181–188, 2022.

[19] B. Banjanin, G. Vladić, M. Pál et al., "Consistency analysis of mechanical properties of elements produced by FDM additive manufacturing technology," *Matéria*, vol. 23, no. 4, 2018.